PHYSICAL REVIEW B, VOLUME 65, 020404(R)

Chemical shift of hyperpolarized ^{129}Xe dissolved in liquid nitrogen

B. Patton, N. N. Kuzma, and W. Happer
Joseph Henry Laboratory, Department of Physics, Princeton University, Princeton, New Jersey 08544
(Received 28 June 2001; published 7 December 2001)

We report NMR measurements of hyperpolarized xenon dissolved in liquid nitrogen. The dependence of the ^{129}Xe frequency shift on liquid nitrogen temperature was measured along the nitrogen saturated vapor curve from 77 to 93 K. Plotted as a function of the liquid nitrogen density, the chemical shift of xenon is very well described by a simple proportionality relation, with a slope of 0.2135(15) ppm/amagat. The relationship between the chemical shift and the longitudinal spin relaxation is considered in terms of the spin-rotation interaction, and estimates of Xe relaxation time in liquid nitrogen are discussed.

DOI: 10.1103/PhysRevB.65.020404 PACS number(s): 76.60.Cq, 32.80.Bx, 64.75.+g

Over the past decade, considerable progress has been made in the area of optical pumping[1] and large-volume production[2,3] of hyperpolarized noble gases. High-resolution ^{3}He images of human lungs have been reported,[4] but the quality of ^{129}Xe lung imaging[5] is still limited by the comparatively low (about 10%) nuclear spin polarization currently achievable in pure xenon.

There have been a number of studies in recent years[6–8] focusing on the physics behind processes taking place in the optical pumping cell, where high-power circularly polarized laser light is absorbed by rubidium vapor atoms which then transfer spin polarization to ^{129}Xe nuclei. However, very little remains known about the physics taking place during the cryogenic separation of spin-polarized xenon from the much larger quantities of buffer gases that are currently admixed with xenon during optical pumping.[2] Despite experimental evidence[9] that a small quantity of xenon preserves its polarization throughout the freeze/thaw cycle in a sealed cell, more than half of the nuclear polarization is currently lost during cryogenic separation in high-volume xenon polarizers.

Given that nitrogen is a key component of the buffer gas mixture, it is important to understand the nature of spin relaxation in xenon-nitrogen mixtures, especially during buffer gas separation. Since a considerable amount of xenon gas dissolves[10] in liquid nitrogen at the cryogenic separation temperature of 77 K, it may be possible to gain insight into the mechanisms of xenon relaxation in condensed nitrogen by examining the relationship between the spin relaxation rate and the chemical shift of ^{129}Xe nuclei.[11,12] Both of these quantities can be measured directly with nuclear magnetic resonance (NMR) spectroscopy, a powerful probe of spin interactions between a nucleus and its local environment.[13]

The first systematic NMR studies of pure xenon date back to the 1960s.[14,15] In the 1970s, C. J. Jameson, A. K. Jameson, and co-workers carried out a number of NMR measurements on xenon mixed with other gases,[16] including a 1978 study[17] of xenon-nitrogen gas mixtures in the temperature range of 220–380 K. *Ab initio* calculations of the ^{129}Xe nuclear magnetic shielding in the Xe–N_2 system were reported by de Dios and C. J. Jameson[18] in 1997.

Here we present NMR measurements of hyperpolarized xenon dissolved in liquid nitrogen. Over the temperature range of 77–93 K at a 1.435-T magnetic field, the chemical shift of ^{129}Xe is found to be very nearly proportional to the liquid nitrogen density. This shift is closely related to the spin-rotation interaction,[19] which is thought to mediate the longitudinal spin relaxation of ^{129}Xe in liquid nitrogen.

In this experiment, xenon gas was polarized with a prototype commercial system (model IGI.9800.Xe polarizer, MITI) connected via a pair of nylon tubes to a glass cold finger, as shown in Fig. 1. The cold finger was placed in a cryostat bore of a superconducting magnet (Oxford Instruments). The apparatus was first evacuated to 5×10^{-3} torr, then flushed and filled with pure (99.9995%+) N_2 gas. The sample space was cooled down and maintained at 64 K (just above the melting point of nitrogen) for half an hour, allowing at least 10 cm^3 of liquid nitrogen (LN_2) to condense in the cold finger. The standard

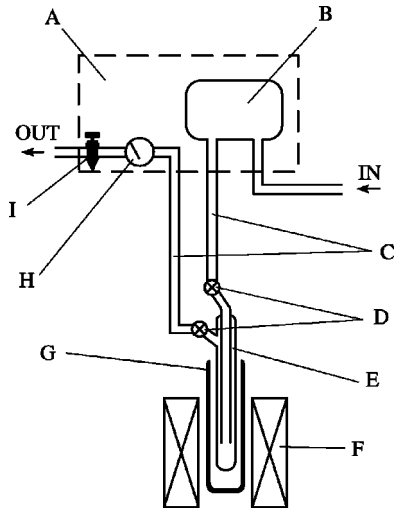

FIG. 1. Schematic diagram of the experimental setup. The He–N_2–Xe gas mixture supplied to the xenon polarizer (A) enters the optical pumping cell (B), which is heated to 175 °C in a 20 G magnetic field. There circularly polarized laser light optically pumps Rb vapor that imparts some of its spin polarization to xenon. The gas mixture containing hyperpolarized ^{129}Xe is then supplied via one of the two nylon tubes (C) to the glass cold finger (E), fitted with shut-off valves (D). The cold finger is placed into the cryostat insert (G), mounted inside a superconducting magnet (F). The gas pressure, monitored by the gauge (H), can be adjusted using the needle valve (I).

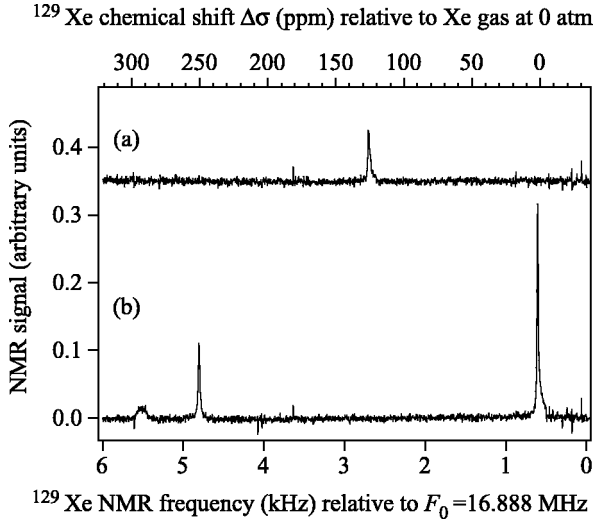

FIG. 2. (a) Representative ^{129}Xe NMR spectrum of hyperpolarized xenon dissolved in liquid nitrogen at 90 K. (b) NMR spectrum of xenon at its triple point (161.35 K, 0.81 atm), where the three peaks (left to right) are due to the solid, liquid, and gaseous phases of xenon. Zero on the bottom scale corresponds to the NMR frequency $F_0 = 16.888$ MHz.

He–N_2–Xe gas mixture ($\sim 1\%$Xe of natural isotopic composition) was then polarized and flowed through the cold finger at a pressure of 4.5 atm. As the warm mixture bubbled through the cold LN_2, the latter boiled off, rapidly increasing the concentration of dissolved xenon. At some point enough hyperpolarized xenon was dissolved to produce detectable NMR signals, with at least 5 cm^3 of LN_2 remaining in the cold finger. Since LN_2 was essentially in equilibrium with N_2 gas, its pressure was a well-defined function of temperature (barring small corrections due to the dissolved Xe). Thus the liquid nitrogen temperature T could be varied either by heating the sample or by depressurizing the cold finger. Two Cernox^{TM} thin-film resistors (model CX-1080-BG-HT, Lake Shore), immersed in the liquid sample 2 cm one above the other, were used as temperature sensors. Occasionally, thermal stratification in the liquid was observed, and a data point was discarded if the two sensors showed a temperature difference $\Delta T > 1$ K. Although both sensors were calibrated to ± 0.1 K, we used ΔT as the temperature error for each NMR measurement.

A two-turn NMR surface coil was mounted around the cold finger in a region where the applied field $B_0 = 1.435$ T was homogeneous to 1.5 parts per million (ppm). The coil was connected to an external resonant tank circuit, tuned to a frequency F_0 close to the Larmor frequency of ^{129}Xe nuclei. A simple homodyne NMR spectrometer supplied short excitation pulses ($5-50$ μs at F_0) to the coil and recorded the subsequent free induction decays (FID) of the ^{129}Xe nuclear magnetization by mixing the amplified signal with the $\sin(2\pi F_0 t)$ and $\cos(2\pi F_0 t)$ waveforms, applying a low-pass filter, and taking the Fourier transform. The absorptive part of the resulting spectrum was plotted as a function of frequency.

Figure 2(a) shows a typical NMR spectrum of xenon dissolved in liquid nitrogen, taken at $T = 90$ K. The motionally narrowed peak is ~ 25 Hz wide due to the homogeneity of the applied field. The relative peak frequency in Fig. 2(a) is 2.7 kHz, which corresponds to the NMR frequency $\nu = F_0 + 2.7$ kHz, with $F_0 = 16.888$ MHz. For comparison, a spectrum of pure xenon at its triple point (161.35 K, 0.81 atm) is shown in Fig. 2(b). NMR lines due to all three phases of xenon (left to right: solid, liquid, gas) are clearly resolved. Their chemical shifts (top scale) are approximately proportional to density, consistent with the early measurements in pure xenon.[14,15]

If attributed to xenon gas, the peak at 127 ppm in Fig. 2(a), roughly half-way between the gas and the liquid lines of Fig. 2(b), would imply a gas density of about 300 amagats,[20] inconsistent with the low pressures in this experiment. The only phase that can exhibit this motionally narrowed ^{129}Xe line at $T < 100$ K is a solution of xenon in liquid nitrogen. This interpretation is consistent with our observations of a second, much broader peak at ~ 300 ppm at the end of the experiment: when saturated, xenon precipitates out as a solid.

To convert the NMR frequency ν into the chemical shift $\Delta\sigma = (\nu - \nu_{g0})/\nu_{g0}$, it was necessary to measure ν_{g0}, the frequency of a reference substance, conventionally defined as pure xenon in the limit of zero density. We obtained ν_{g0} in two steps: First, the NMR frequency of ^{129}Xe in the He–N_2–Xe gas mixture was monitored at room temperature and 4.5 atm immediately before and after each cryogenic experiment. From these room temperature data, a small (on the order of 1 ppm) and fairly reproducible magnetic field drift in the superconducting magnet was interpolated as a function of time, and the cryogenic NMR data were thus referenced to the frequency of xenon in the gas mixture. The error of this interpolation and the 1.5 ppm linewidth of the NMR signals determined the error of the chemical shift measurements. Second, the frequency of xenon in the gas mixture at 4.5 atm was compared to the frequency of pure xenon gas (polarized and cryogenically separated in another cold finger), measured at room temperature and 1.6 atm. Using the known dependence of the chemical shift on density in pure xenon,[14] it was found that the NMR frequency of xenon in the 4.5 atm gas mixture was equal, within errors, to ν_{g0}. This is consistent with expectations based on the known chemical shifts of xenon mixed with nitrogen[17] and other gases.[16] Other possible systematic errors (such as thermal displacement of the coil relative to the magnet, presence of paramagnetic contaminants that could cause temperature-dependent field shift and distortion, effects of the heater current on the NMR frequency and line shape, or condensation of paramagnetic liquid oxygen on the outer surface of the cold finger) were carefully examined and eliminated. The narrow NMR line of the dissolved xenon and the reproducibility of the chemical shifts over eight cryogenic cycles are good indications of the validity of our data.

Figure 3 shows the chemical shift $\Delta\sigma$ of dissolved ^{129}Xe, measured as a function of temperature T (top scale). Neglecting the small corrections due to dissolved xenon, the density ρ_{N_2} of the liquid (bottom scale) was calculated using the

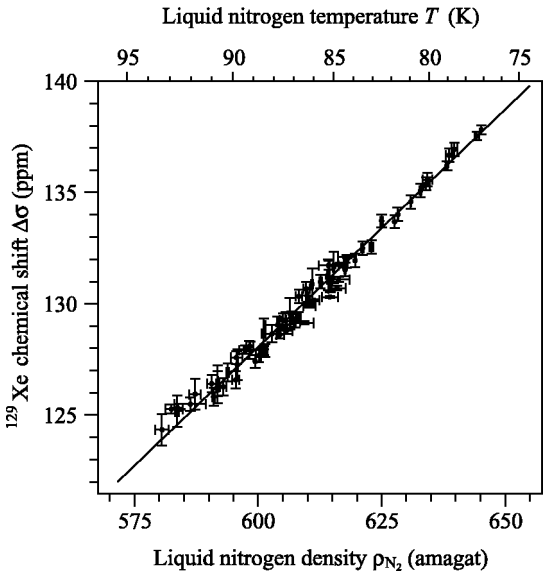

FIG. 3. ^{129}Xe chemical shift $\Delta\sigma$ of xenon dissolved in liquid nitrogen measured as a function of temperature (nonuniform top scale) along the saturated pressure curve. The temperature of liquid nitrogen was converted into density ρ_{N_2} (linear bottom scale) using Ref. 19. The solid line is a one-parameter fit $\Delta\sigma = k_1\rho_{N_2}$, with the fitting constant $k_1 = (0.2135 \pm 0.0015)$ ppm/amagat.

published liquid-vapor equilibrium data $\rho_{N_2}(T)$ for nitrogen.[21] The temperature range covered, 77–93 K, corresponds to the equilibrium nitrogen vapor pressures of 1–4.5 atm. The solubility of xenon in liquid nitrogen is a strong function of temperature, which we approximate from published experimental data[10] as

$$x(T) = \exp\left(3.288 - \frac{761.5\ \mathrm{K}}{T}\right) \pm 2\times 10^{-3} \quad \text{for} \quad 91 < T < 127.3\ \mathrm{K}, \tag{1}$$

where $x = [\mathrm{Xe}]/[\mathrm{Xe}+\mathrm{N_2}]$ is the molar fraction of dissolved xenon. Extrapolating Eq. (1) to 77 K, we obtain $x(77\ \mathrm{K}) = 1.4\times 10^{-3}$, compared to $x(93\ \mathrm{K}) = 7.4\times 10^{-3}$. This is why it was more difficult to obtain signal at lower temperatures. On the other hand, measurements around 93 K yielded good signals, but were limited to 4.5 atm by the estimated mechanical strength of the glass.

All of the data in Fig. 3 are well described by the one-parameter fit $\Delta\sigma = k_1\rho_{N_2}$ (solid line), with

$$k_1 = (0.2135 \pm 0.0015)\ \ \mathrm{ppm/amagat}. \tag{2}$$

Figure 4 compares the experimentally measured values of this constant for xenon dissolved in liquid (present work) and gaseous nitrogen[17] to the results of recent *ab initio* calculations for the Xe–N_2 system.[18] The calculations seem to reproduce the gaseous data qualitatively (note the minimum in k_1 at 250 K, which occurs at 300 K in the calculation), although good quantitative agreement has yet to be achieved.

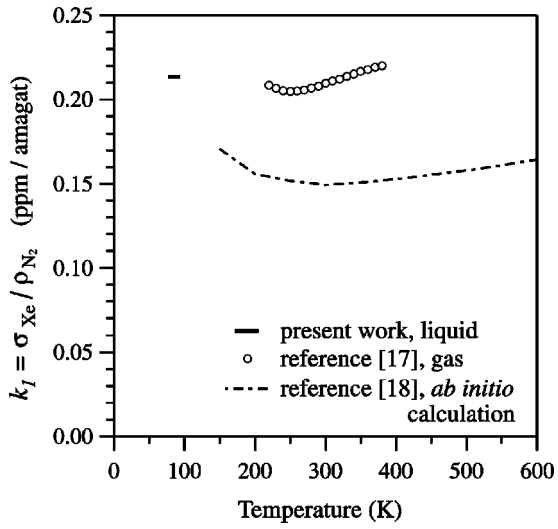

FIG. 4. Comparison of the proportionality constants $k_1 = \Delta\sigma/\rho_{N_2}$ (the ratio of the chemical shift to the nitrogen density) for xenon dissolved in liquid and gaseous nitrogen.

The challenges associated with *ab initio* calculations of intermolecular chemical shifts are well described in a review by de Dios.[22]

Relatively large chemical shifts $\Delta\sigma$ of xenon, such as plotted in Fig. 3, can be explained in terms of the spin-rotation interaction[12] between a ^{129}Xe nucleus and neighboring atoms. For gaseous xenon, Torrey[11] showed that

$$\Delta\sigma = \frac{2}{3}\frac{\mu_B}{\hbar}\left\langle\frac{H_r(\omega)}{\omega}\right\rangle, \tag{3}$$

where $H_r(\omega)$ is the field induced at the ^{129}Xe nucleus by the rotation of a Xe-Xe pair with angular velocity ω, and μ_B is the Bohr magneton. The average denoted by $\langle \ldots \rangle$ is taken over all configurations of the nearest neighbors.

In a clean diamagnetic system of dilute spin-1/2 nuclei, the longitudinal relaxation rate $1/T_1$ at moderate magnetic fields (0.2–10 T) is often attributed[23] to the spin-rotation field $H_r(\omega)$. Using the rigid-sphere approximation, Torrey obtained for xenon gas:

$$\frac{1}{T_1} = \frac{21}{40\pi}\left(\frac{\mu_{Xe}}{\mu_B}\right)^2 \frac{\overline{v_r}}{nR_m^4}(\Delta\sigma)^2, \tag{4}$$

where μ_{Xe} is the magnetic moment of the ^{129}Xe nucleus, $\overline{v_r} = (8kT/\pi m_r)^{1/2}$ is the mean relative velocity of a Xe-Xe pair, m_r is its reduced mass, $R_m = 3.32$ Å is the effective rigid sphere diameter, and n is the number density of atoms. Equation (4) was modified by Oppenheim *et al.*[24] for the case of liquid xenon:

$$\frac{1}{T_1} = \frac{128\pi}{3}\left(\frac{\mu_{Xe}}{\hbar}\right)^2 nD\int_0^\infty g(R)\left(\frac{H_r(\omega)}{\omega}\right)^2 dR, \tag{5}$$

where D is the diffusion coefficient of xenon in the liquid and $g(R)$ is the radial density distribution function, normalized to $g(\infty) = 1$. The term $H_r(\omega)/\omega$ depends on R and is the same as in Eq. (3). The measurements in pure xenon liquid

by Sauer *et al.*,[25] who obtained $T_1 \approx 0.5$ h at $T = 165$ K, are in fairly good agreement with Eq. (5). Assuming the quantities n, D, and $g(R)$ are comparable for liquid xenon at 165 K and for a Xe–N_2 solution at ~ 90 K, the $\Delta\sigma$ data in Fig. 2(a,b) would imply for the Xe–N_2 system a value of $T_1 \sim 2$ hours.

In practice, we could not observe any NMR signals of dissolved xenon several minutes after the gas flow from the polarizer was stopped. As a cross-check, we polarized a batch of pure xenon liquid in our apparatus, and obtained a T_1 value of ~ 18 min, in line with Sauer's data.[25] However, we cannot conclude that the T_1 of xenon in liquid nitrogen is much shorter than that predicted by Eq. (5), since changes in Xe concentration during the experiment can lead to a disappearance of Xe NMR signal. Currently, it is not possible to distinguish between ^{129}Xe relaxation and variations in Xe concentration in our relatively low-field apparatus.

We thank Bastiaan Driehuys for many helpful discussions and for the loan of the superconducting magnet system. We also thank Michael Souza for his help with the cold finger design and Jacob Goldston for participation in setting up the apparatus. This work was supported by the U.S. Air Force Office of Scientific Research.

[1] T.G. Walker and W. Happer, Rev. Mod. Phys. **69**, 629 (1997).
[2] B. Driehuys, G.D. Cates, E. Miron, K. Sauer, D.K. Walter, and W. Happer, Appl. Phys. Lett. **69**, 1668 (1996).
[3] J.R. Johnson *et al.*, Nucl. Instrum. Methods Phys. Res. A **356**, 148 (1995); T.E. Chupp, M.E. Wagshul, K.P. Coulter, A.B. McDonald, and W. Happer, Phys. Rev. C **36**, 2244 (1987).
[4] H.-U. Kauczor, *et al.*, J. Magn. Reson. Imaging **7**, 538 (1997); E.E. de Lange *et al.*, Radiology **210**, 851 (1999).
[5] J.P. Mugler *et al.*, Magn. Reson. Med. **37**, 809 (1997).
[6] D.K. Walter, W.M. Griffith, and W. Happer, Phys. Rev. Lett. **86**, 3264 (2001).
[7] C.J. Erickson, D. Levron, W. Happer, S. Kadlecek, B. Chann, L.W. Anderson, and T.G. Walker, Phys. Rev. Lett. **85**, 4237 (2000).
[8] S. Appelt, A.B. Baranga, A.R. Young, and W. Happer, Phys. Rev. A **59**, 2078 (1999).
[9] G.D. Cates, D.R. Benton, M. Gatzke, W. Happer, K.C. Hasson, and N.R. Newbury, Phys. Rev. Lett. **65**, 2591 (1990); U. Ruth, T. Hof, J. Schmidt, D. Fick, and H.J. Jansch, Appl. Phys. B: Lasers Opt. **68**, 93 (1999).
[10] M. Teller and H. Knapp, Cryogenics **24**, 471 (1984).
[11] H.C. Torrey, Phys. Rev. **130**, 2306 (1963).
[12] N.F. Ramsey, Phys. Rev. **78**, 699 (1950).
[13] C.P. Slichter, *Principles of Magnetic Resonance* (Springer-Verlag, Berlin, 1990).
[14] R.L. Streever and H.Y. Carr, Phys. Rev. **121**, 20 (1961); E.R. Hunt and H.Y. Carr, *ibid.* **130**, 2302 (1963); D. Brinkmann and H.Y. Carr, *ibid.* **150**, 174 (1966); D. Brinkmann, Phys. Rev. Lett. **13**, 187 (1964); E. Kanegsberg, B. Pass, and H.Y. Carr, *ibid.* **23**, 572 (1969).
[15] W.Y. Yen and R.E. Norberg, Phys. Rev. **131**, 269 (1963); W.W. Warren and R.E. Norberg, *ibid.* **154**, 277 (1967); D.F. Cowgill and R.E. Norberg, Phys. Rev. B **6**, 1636 (1972).
[16] A.K. Jameson, C.J. Jameson, and H.S. Gutowsky, J. Chem. Phys. **53**, 2310 (1970); C.J. Jameson and A.K. Jameson, Mol. Phys. **20**, 957 (1971); C.J. Jameson, A.K. Jameson, and S.M. Cohen, J. Chem. Phys. **59**, 4540 (1973); **62**, 4224 (1975); **65**, 3397 (1976); **65**, 3401 (1976); Mol. Phys. **29**, 1919 (1975).
[17] C.J. Jameson, A.K. Jameson, and H. Parker, J. Chem. Phys. **68**, 3943 (1978).
[18] A.C. de Dios and C.J. Jameson, J. Chem. Phys. **107**, 4253 (1997).
[19] R.J. Fitzgerald, M. Gatzke, D.C. Fox, G.D. Cates, and W. Happer, Phys. Rev. B **59**, 8795 (1999).
[20] An amagat is defined as the number density of an ideal gas at 0 °C and 1 atm. (273.15 K and 101325 Pa). It is equal to the Loschmidt constant, 2.6868×10^{19} cm^{-3}.
[21] V.V. Sychev, A.A. Vasserman, A.D. Kozlov, G.A. Spiridonov, and V.A. Tsymarny, *Thermodynamic Properties of Nitrogen* (Hemisphere Publishing, Washington, 1987).
[22] A.C. de Dios, Prog. Nucl. Magn. Reson. Spectrosc. **29**, 229 (1996).
[23] H.W. Spiess, D. Schweitzer, U. Haeberlen, and K.H. Hausser, J. Magn. Reson. (1969-1992) **5**, 101 (1971).
[24] I. Oppenheim, M. Bloom, and H.C. Torrey, Can. J. Phys. **42**, 70 (1964).
[25] K.L. Sauer, R.J. Fitzgerald, and W. Happer, Chem. Phys. Lett. **277**, 153 (1997).